J. Fluid Mech. (1979), *vol.* 91, *part* 1, *pp.* 41–63
Printed in Great Britain

A fluid-mechanical study of the closure of heart valves

By C. S. F. LEE AND L. TALBOT
Department of Mechanical Engineering, University of California, Berkeley

(Received 15 September 1977 and in revised form 25 August 1978)

The fluid mechanics of heart-valve motion is investigated experimentally and theoretically. From the experiments, it is found that the principal mechanism ensuring optimal mitral-valve closure is the pressure field induced by a strong flow deceleration through the valve. A complete theory, evolved from the Bellhouse & Talbot analytical model, is developed for both the mitral and the aortic valve to provide a relationship between valve motion and valve flow. Results predicted by this theory agree consistently well with those obtained from experiments.

1. Introduction

In their healthy state, the valves of the heart are remarkably efficient devices, offering very little resistance to flow when open, and capable of closing in response to small pressure differences and with a negligible amount of regurgitated flow. They are essentially passive organs whose motions are due mainly to the fluid-dynamical forces exerted upon them, and for this reason the analysis of these forces is a requisite for understanding the functioning of the valves in both healthy and diseased states. The valves are of two types: the atrioventricular valves (tricuspid and mitral), which separate the atria and ventricles of the right and left heart, and the semilunar valves (pulmonic and aortic), which regulate the outflow from the right and left ventricles. Our discussion here will focus on the aortic and mitral valves of the left heart, but our general conclusions will be equally applicable to the tricuspid and pulmonic valves.

The aortic valve consists of three thin crescent-shaped cusps (whence the name semilunar) which in the open position are displaced outwards to line up approximately with the portion of the aorta distal to the valve. In the closed position the adjacent distal margins of the three cusps come together along three radii 120° apart to seal the aortic orifice. Behind the cusps the aortic root forms bulges called the sinuses of Valsalva, which, as reported by Bellhouse & Talbot (1969), play a role in the closure mechanism of the valve. The pulmonic valve has a similar structure.

The mitral valve consists of two main thin membranous cusps of roughly trapezoidal shape which originate from the slightly elliptical mitral ring to form in the open position a truncated and scalloped cone-like structure. The distal margins of the two cusps have an irregular appearance owing to the insertion of the chordae tendineae (string-like fibrous structures connecting the valve cusps to the ventricular wall), which originate from the papillary muscles of the ventricular wall. The cusp adjacent to the aortic valve is designated as the anterior or aortic cusp while the one closer to the ventricular wall is designated as the posterior or mural cusp. On closure, the

0022-1120/79/4175–5890 $02.00

free edge of one cusp is pressed against that of the other to seal the valve. The morphology of the tricuspid valve is similar to that of the mitral valve, except that three major cusps can be identified. Beautiful illustrations of all four valves of the heart can be found in Netter (1974).

Owing to frequent diagnosis of valvular incompetence in association with cardiopulmonary malfunctions, the motions of heart valves have attracted a considerable amount of attention on the part of physiologists and physicians. In fact, the first to explore the nature of heart-valve operation were two physiologists, Henderson & Johnson (1912), who used simple yet illustrative *in vitro* experiments which provided fairly accurate descriptions of the dynamics of valve closure. They described the closure mechanism as a 'breaking of a jet', although they recognized that the mechanism they described was due to 'pressure produced within the ventricles by the inertia of the jet'. As illustrated in figure 1, in one of their experiments dye was allowed to run down along tube A into a large reservoir B within which a jet of dye was visible. As the flow in A was halted, the jet in B conserved its forward motion and hence broke away from the fluid in tube A while clear water around the jet was drawn suddenly into its wake in the vicinity of the tube opening. When a flexible sleeve was attached to the end of the tube, the inward-moving reservoir fluid caused the sleeve to collapse and seal the tube. Regrettably, their conclusions were for the most part unappreciated or misinterpreted by subsequent researchers.

Fluid-dynamical investigations of heart-valve motions were reported by Bellhouse & Bellhouse (1969, 1972). From their two consecutive model experiments on the motions of aortic and mitral valves, conclusions were derived with a view somewhat different from that of Henderson & Johnson. Whereas Henderson & Johnson stated that efficient valve closure could be accomplished by cessation of flow through the valve orifice in the absence of eddy motion, Bellhouse & Bellhouse stressed that, in addition to flow deceleration through the valves, vortical flow which developed around heart valves before their closure played an essential role in optimal valve functioning. Though no deficiency has been found in the concepts of Henderson & Johnson, many present researchers appear to favour the Bellhouse & Bellhouse 'vortex' theory. It may be remarked however that there is no fundamental disagreement in fluid-dynamical principles between the Henderson–Johnson and Bellhouse approaches. Explanations of fluid motions in terms of momentum–pressure arguments or vorticity arguments can be equally valid, and it is generally a matter of personal preference and convenience as to which one is used; some situations lend themselves more naturally to one, some to the other. The only question is whether the flow model, be it a vorticity or a pressure–momentum one, predicts accurately the behaviour of the physical flow.

Lee (1977) pointed out that some of the observations made from the Bellhouse & Bellhouse experiments were not entirely conclusive. In brief, their aortic experiment did not completely verify the importance of the sinus vortex in valve closure because the effect of viscosity in inhibiting flow behind the valve cusps in their sinus-less valve was not considered. The existence of this uncertainty was further supported by the report of Bellhouse *et al.* (1973) and that of Spaan *et al.* (1975). In the Bellhouse & Bellhouse investigation of mitral-valve functioning, the observation that valve closure was delayed when the ventricular volume was increased was attributed to a decrease in strength of the ventricular vortex in valve closure. However, the same

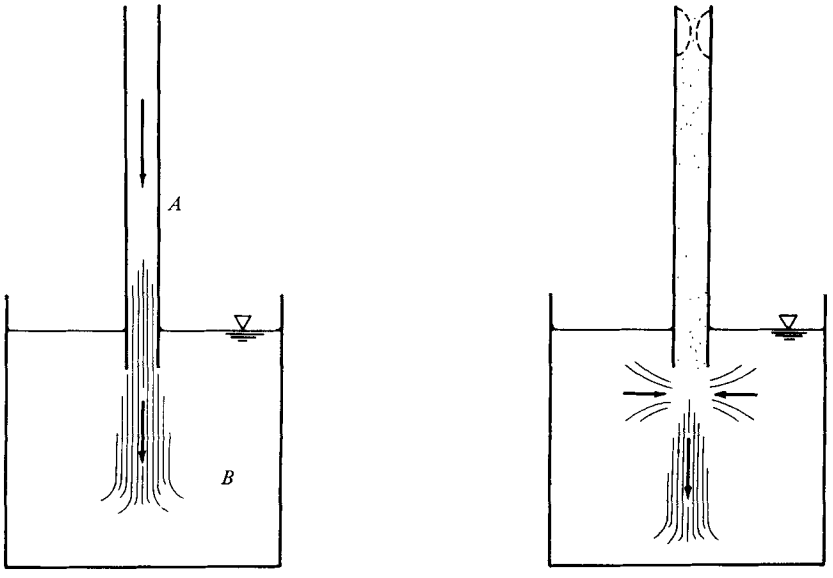

FIGURE 1. The experiment of Henderson & Johnson (1912). (*a*) An initially steady jet. (*b*) The ' breaking of a jet ' phenomenon occurred after the tube was pinched.

conclusions can be reached concerning the relationship between valve response and ventricular volume for other assumed velocity distributions within the ventricle, as for example, the assumption of uniform kinetic energy density.

The theory developed by Bellhouse & Talbot (1969) was the first mathematical approach making use of fluid-dynamical principles to describe aortic-valve functioning. A vortical flow field in the form of the classical Hill spherical vortex was assumed for the fluid motion in the aortic sinuses. The analysis was found to be quite successful in predicting the pressure differences across the cusp when compared with those measured in the model experiment of Bellhouse & Bellhouse (1969). However, they did not attempt to solve for the theoretical valve motion although the theory could be used to do so. The theory of Bellhouse & Bellhouse derived for the calculation of mitral-valve motion was essentially the same model as was used by Bellhouse & Talbot for the aortic valve. The results of their study suggested that the theory qualitatively described mitral-valve behaviour, but some improvements in its accuracy were required for any further practical application. Peskin (1972), on the other hand, carried out numerical analysis of the full equations of motion, for a two-dimensional model of the ventricle, without making any *a priori* assumptions as to the structure of the flow. Although his results cannot be directly applied to model or physiological experiments because of the two-dimensionality of his analytical model, they do show some very interesting details of the flow field within the ventricle, such as the 'breaking of the jet' phenomenon during valve closure. In his numerical experiments, Peskin found that it was necessary to provide mathematical constraints on the valve cusps in order to prevent them from opening too much. This condition was not observed in the Bellhouse & Bellhouse experiment. It should be pointed out that computational limitations restricted Peskin's calculations to a rather low

Reynolds number, in contrast to the higher values in the physiological range used in the Bellhouse & Bellhouse experiment. At low Reynolds numbers jets issuing from orifices diverge farther than at high Reynolds numbers, which may be the explanation for these different conclusions concerning the role of the chordae tendineae in providing restraints on valve cusp motion.

We present in the following a portion of our experimental studies on the motion of the mitral valve in an attempt to resolve some of the questions mentioned earlier. Guided by the results of these experiments, the original Bellhouse & Talbot theory was modified such that theoretical calculation of mitral- or aortic-valve motion can be achieved with higher accuracy. Moreover, the influences on mitral-valve behaviour of specific physical parameters are also demonstrated using the modified theory. The clinical importance of an accurate theoretical model should be noted. As will be reported elsewhere, we have found that it is possible from our theory to predict the flow through heart valves, and hence measure cardiac output, from echocardiographic measurements of valve motion.

2. Experiment

A mechanical model bearing geometrical and dynamical similarity to a typical human left heart was employed in our experimental investigations, which are reported in detail by Lee (1977). As illustrated in figure 2, the focal point of our experiment was the ventricle of the heart model, which was connected to a compliance–resistance mock circulatory network. Plexiglas and clear silicone rubber were selected as the materials for the model owing to their optical transparency, which facilitated flow visualization. The aortic-valve prototype, which had a leak factor of only 4 ml per 100 ml stroke volume, resembled closely the one described by Bellhouse & Bellhouse (1969). The competence of this valve was necessary to ensure disturbance-free motion of the anterior mitral leaflet because aortic regurgitation is known to induce abnormal early closure of this cusp. Several mitral-valve prototypes were tested before we finally reached a satisfactory design for a fairly two-dimensional model, as shown in figure 3. This mitral valve consisted of two rigid Plexiglas valve cusps which were mounted on a frame provided with parallel triangular side walls and containing a round orifice. The valve hinges were made of very flexible thin plastic sheeting and permitted the cusps to open to well beyond an included angle of 180°. Apart from their hinges, the cusps were unconstrained. Compressed air and a vacuum formed the power source for the synchronous pumping actions of the atrium and ventricle, through the control of a dual electronic pneumatic heart pump that allowed variation of the heart rate, systole-to-diastole time ratio, contractility and atrial systole-to-ventricular systole time interval. This model, whose dynamics are shown in figure 4, was found to be quite successful in duplicating physiological pressure and flow wave forms.

For a pulsatile system such as our heart model, dynamical similarity requires the Reynolds number $Re = UL/\nu$ and Strouhal number $S = L/UT$ of the model to match those of the human system, where U is a typical velocity of the system, L is a typical dimension, T is the period of the heart cycle and ν is the kinematic viscosity of the circulating fluid. We shall use the subscripts p and m to denote the physiological system and the model respectively. Since L_p was equal to L_m by design and T_p was

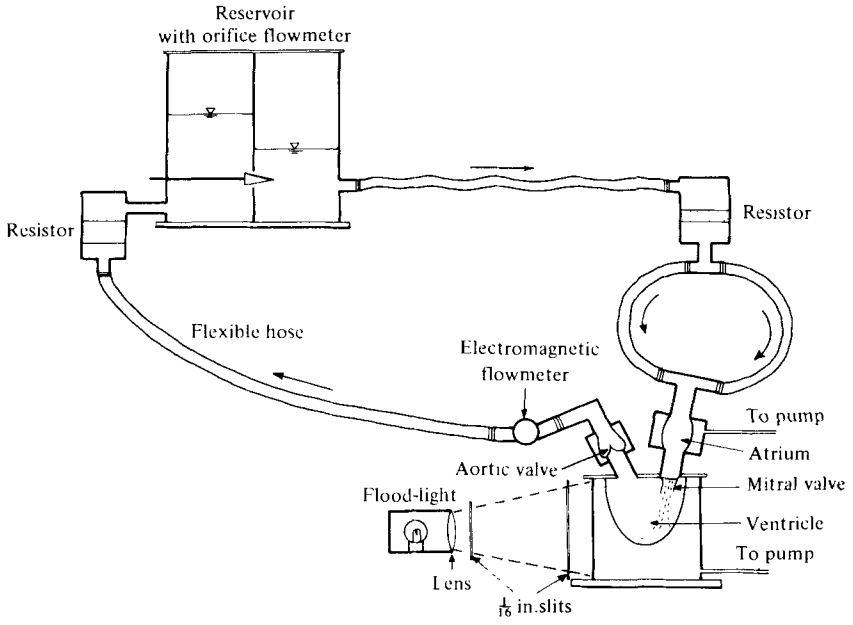

FIGURE 2. Schematic diagram of the model left heart and circulatory network.

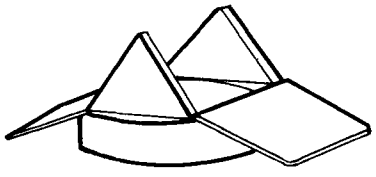

FIGURE 3. Schematic diagram of the model mitral valve.

chosen equal to $T_m/3{\cdot}5$ from preliminary tests (model frequency 20 beats/min and human sinus rhythm 70 beats/min), the conditions $Re_p = Re_m$ and $S_p = S_m$ could be satisfied if and only if $\nu_p = 3{\cdot}5\nu_m$ and $U_p = 3{\cdot}5U_m$. Hence a fluid with a viscosity 3·5 times less than that of blood was needed. Furthermore, the application of electromagnetic flowmetry and hydrogen-bubble flow-visualization necessitated an ionic solution. Saline meets these two criteria and it was therefore chosen as the working fluid. The requirement $U_p = 3{\cdot}5U_m$ was automatically satisfied since $U \propto$ stroke volume/(period × area).

The hydrogen-bubble technique employed for flow visualization is shown schematically in figure 2. We focused our attention mainly on the time-varying two-dimensional flow patterns observed on the 'plane of symmetry' (the geometrically defined plane which vertically divided the ventricle into two equal halves along the atrial–aortic orientation). The ventricular-wall motion, mitral-valve motion and bubble movements, which represented local fluid velocities, were recorded on 16 mm film by high-speed cinematography using a Redlake Locam movie camera at 100 frames/s, as well as on 35 mm stills taken with a Topcon SLR camera equipped with an electronic variable-delay camera shutter control which was synchronized with the pneumatic pump. In order to reference the timing of the valve movements, two small lights

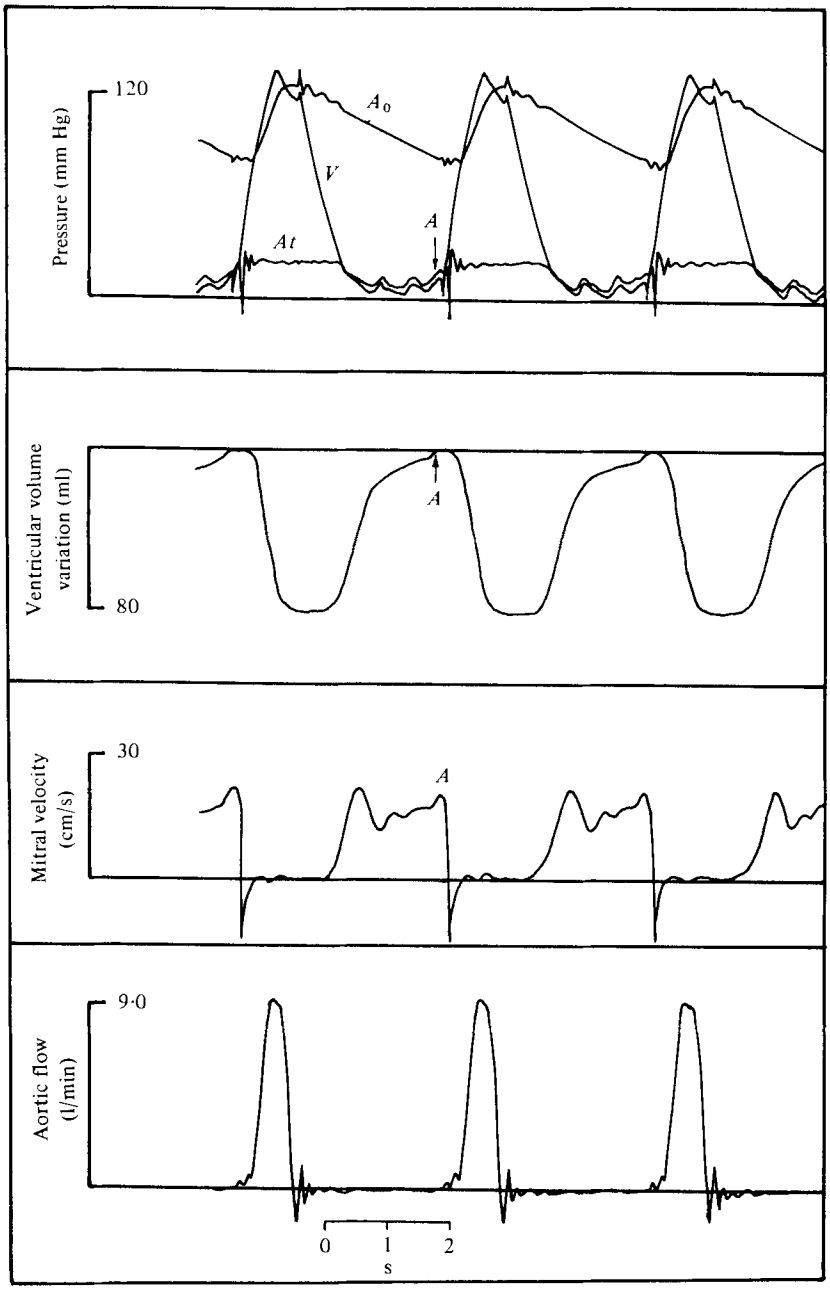

FIGURE 4. The dynamics of the experimental system operated under typical conditions; heart rate = 18 beats/min, systole-to-diastole time ratio = $\frac{1}{2}$ and stroke volume = 80 ml. A_0 denotes aortic pressure, V ventricular pressure, At atrial pressure and A atrial contraction.

electronically triggered by the onset of the ventricular and atrial pumps respectively were also recorded on the films. The films were analysed on a Vanguard Motion Analyzer and the resulting digitized data were finally reduced using a CDC 6400 computer. Special computer codes were developed to correct for optical refractive distortions in the visual locations of the bubbles and of the mitral-valve cusps within the inverted-bell-shaped ventricle, as well as to carry out the integration for the ventricular volume using its shape profile obtained from the film records. Because of the axial symmetry of the model ventricle, this volume calculation was found to be sufficiently accurate to permit determination of the amount of regurgitation which occurred during mitral-valve closure.

In addition to the photographic methods, pressure and flow measurements were recorded on an eight-channel strip-chart recorder (Beckman RM Dynagraphic) using standard equipment such as a Miller catheter-tip pressure gauge, Hewlett–Packard differential pressure transducers 276BC, and a directionally sensitive square-wave electromagnetic flowmeter (Carolina Medical Electronics, Inc.) incorporating an extracorporeal probe and a catheter-tip velocity probe.

Our first experiment was to explore the nature of pulsatile flow through the mitral orifice and within the ventricle, with and without a mitral valve. As shown in figure 5 (plate 1, without a mitral valve) and figure 6 (plate 2, with a mitral valve), two series of photographs were taken under the same experimental conditions (heart rate 20 beats/min, stroke volume 80 ml, systole-to-diastole time ratio $\frac{1}{2}$, peak velocity 20 cm/s and no atrial contraction). One can observe appreciable similarities between these two cases, for example the formation of a smoke-ring-type starting vortex, the early descent of this vortex to the lower and outer portion of the ventricle, the straightness of the fully developed mid-diastolic jet, which was surrounded by relatively stationary fluid, and the 'breaking of the jet' phenomenon after the onset of flow deceleration. From this observation, it is apparent that the 'breaking of the jet' phenomenon is indeed an intrinsic property of pulsatile flow through an orifice. These similarities suggest that valve cusps can be viewed as passive devices which 'float' in response to local fluid motions. The circulatory fluid motion observed in the ventricle after the onset of flow deceleration is probably the consequence of the adverse pressure gradient associated with the decelerating flow in the jet. This pressure field, which is also impressed on the relatively stationary fluid around the jet, would tend to move fluid upwards and then inwards behind the cusps, thereby forming a pattern of flow similar to a vortex, as envisioned in the Bellhouse model. (Whether this flow pattern is the result rather than the cause of the 'breaking of the jet' phenomenon is really more a matter of semantics than fluid mechanics.)

It can be seen from figure 6(*b*) that the starting vortex generated at the time of valve opening is confined to the lower and outer portion of the ventricle throughout the period of quasi-steady mid-diastolic flow. During this period, there is no significant fluid motion behind the valve cusps, which themselves exhibit little movement. However, at about 50–100 ms after the onset of flow deceleration, as seen in figure 6(*c*), motion in the ventricle towards the valve cusps is initiated as they begin to close. The overall appearance of the flow within the ventricle is now circulatory, similar to that proposed by Bellhouse & Bellhouse. However, this circulatory motion is not due to the starting vortex, but rather, as mentioned above, connected with the pressure field which causes the deceleration of the jet flow through the valve since the diffusion

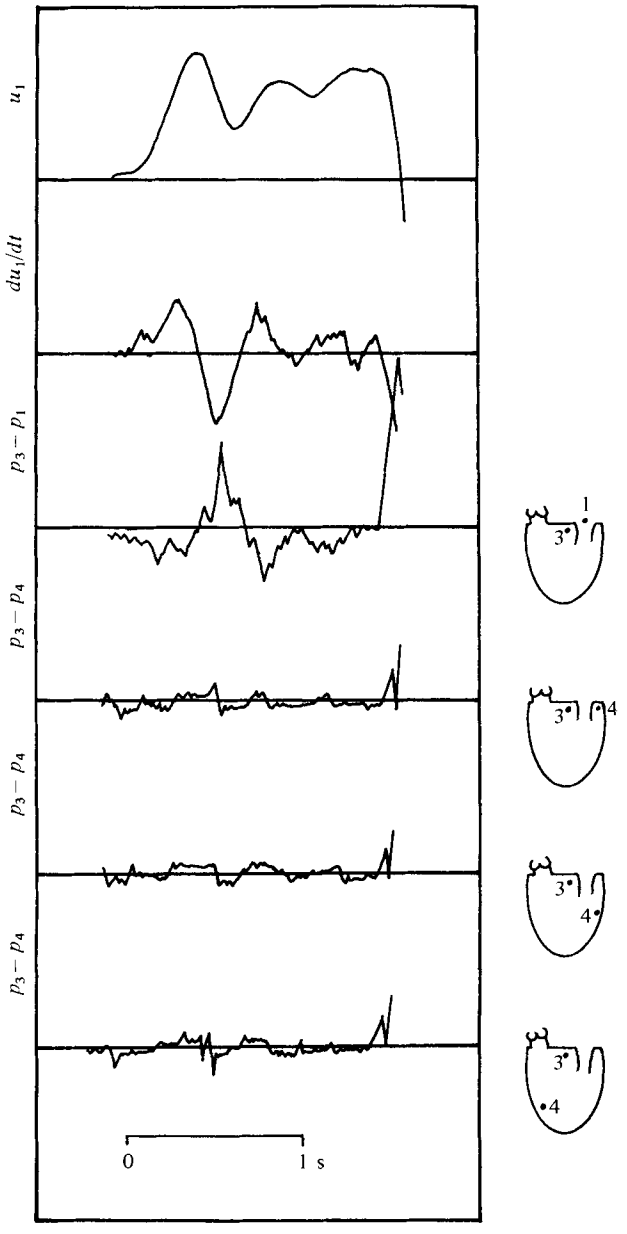

FIGURE 7. Flow deceleration at valve orifice and hydrodynamical pressure differences measured at specified locations inside the ventricle.

time necessary for the existing starting vortex to expand to fill the ventricle is of the order of several hundred seconds.

It may be observed, as was also concluded by Bellhouse & Bellhouse (1972), that the closure mechanism operates efficiently without the need for forces applied to the free margins of the mitral-valve cusps, such as might be provided by chordae tendineae. Nor do restraints appear to be necessary to prevent over-opening of the valve, since the valve cusps align themselves with the boundaries of the nearly parallel jet issuing

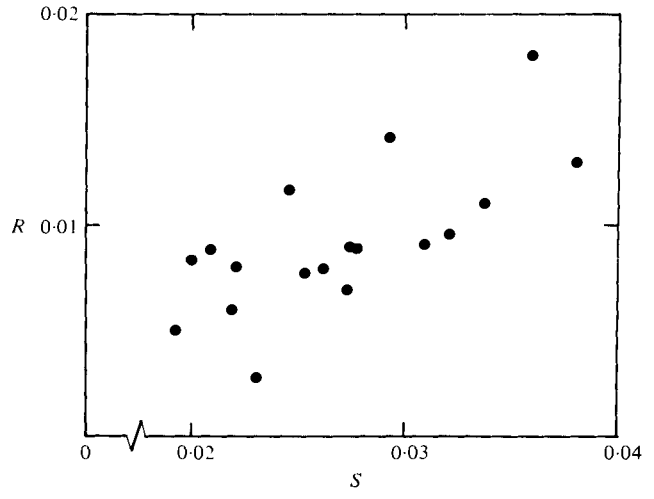

FIGURE 8. Effect of Strouhal number S on mitral regurgitation R.

from the valve in mid-diastole. In case of the physiological valve, the chordae tendineae are necessary to prevent mitral prolapse during ventricular systole, but we do not feel that they contribute actively to the closure process under normal physiological conditions.

The hydrodynamical pressure-difference measurements (hydrostatic pressure variations have been subtracted out) across the aortic cusp and throughout the entire ventricle, when compared with the time derivative of the mitral orifice velocity, as shown in figure 7, provided further evidence to support our view that flow deceleration is the dominant agent for optimal valve closure. It is apparent that very little pressure variation occurred in the fluid behind the cusps and outside the diastolic jet, but more appreciable pressure differences were registered between positions behind the cusps and the mitral orifice and were roughly proportional to the measured flow decelerations.

The effect of flow deceleration was then studied by separately varying the active diastolic period, heart rate and stroke volume. To summarize the results of these studies non-dimensionally, we define a Strouhal number $S = l/U_{\max} T$ and a dimensionless regurgitation index $R = V_b/\pi a^2 U_{\max} T$, where l is the valve length in cm, $U_{\max}$ is the peak velocity at the mitral orifice in cm/s, T is the period of the cardiac cycle in seconds, a is the orifice diameter in centimetres and V_b is the backflow volume in millilitres measured in the tests during valve closure. The data obtained are plotted in figure 8. One observes that, despite the considerable amount of scatter, there is a positive correlation between S and R.

Investigations were also carried out of the effect of ventricular volume on valve closure. The results showed that valve closure was slightly delayed by an increase in ventricular volume. Similar results were reported by Bellhouse & Bellhouse (1972). However, in contrast to their inference that the delay in closure might intensify the amount of regurgitation, we found little change in valve efficiency. In our experiments, the pressure variation around the jet inside the ventricle was found to be of the order of 0·1 torr, whereas the pressure difference between positions behind the valve cusps and the mitral orifice was of the order of 1 torr. In other words, we had a deceleration-dominated valve closure, and the effects of changes in the ventricular

volume were negligible. In the Bellhouse experiment, however, the dimensionless flow deceleration through the valve was consistently lower than that in our tests, and in fact in the early stages of valve closure the deceleration-actuated pressure difference $p_3 - p_1$ across the valve cusps was of the same order of magnitude as the pressure difference $p_3 - p_4$ within the ventricle. An increase in ventricular volume results in a decrease in $p_3 - p_4$. Since in the Bellhouse experiments the contribution of the pressure difference $p_3 - p_4$ to an overall typical pressure difference $p_4 - p_1$ between the ventricle and the orifice was larger than in our experiments, it is not surprising that they observed larger changes in valve closure with changes in ventricular volume than we did. In the case of physiological valves, however, flow deceleration normally occurs quite abruptly and is relatively high, therefore we anticipate no significant effects on the valve functioning due to variations in ventricular end-diastolic volume within its physiological range 100–300 ml.

3. Theory

Our experimental investigations have pointed the way to several possible modifications to the Bellhouse & Bellhouse (1972) theoretical model for the mitral valve, which was evolved from the Bellhouse & Talbot (1969) aortic-valve theory. First, we found that the Bellhouse inviscid model fails to predict the valve opening process. The differential equation based on mass, momentum and energy balances for quasi-one-dimensional inviscid flow which is obtained by Bellhouse & Bellhouse for the opening process possesses a singularity at $\lambda = 0$, the initial condition for the opening (see below). When we avoided this singularity by using experimental data to start the integration at a later time where λ was finite (typically $\lambda = 0{\cdot}1$ and $0{\cdot}2$), the solution $\lambda(\tau)$ for valve cusp position *vs.* time was found to overshoot the actual fully opened configuration by as much as 30 %. This was not the result of a defect in the numerical integration scheme, since we used a fourth-order Runge–Kutta method and obtained satisfactory convergence.

We believe that the reason why the inviscid model fails to predict adequately the valve opening process is that viscous effects play a central role in this process. We noted earlier the similarities in the starting flow through the mitral orifice with and without a valve (figures 5 and 6). In both instances the jet entering the ventricle was essentially parallel (non-divergent), evidently because of flow separation at the orifice. Since separation is a viscous phenomenon not accounted for in the inviscid analysis, it is not surprising that the inviscid model of valve opening does not give satisfactory results. To describe the opening process adequately, one might attempt to formulate a model including viscous effects, but this would be difficult. We have chosen therefore to represent the effect of viscosity in the opening process in terms of its consequences: the essential parallelism of the jet, which leads to the assumption that during valve opening the velocity u_2 at the free margins of the valve cusps is approximately equal to the velocity u_1 at the valve orifice. This assumption together with continuity relations leads to a simple yet accurate description of the opening process.

During valve closure, however, viscous effects appear not to play a significant role. The flow configuration during closure is that of a convergent channel, and the Reynolds number based on channel width at the start of closure is of the order of 5000. Hence

the boundary layers formed on the interior surfaces of the valve cusps will be thin compared with the channel width, and the flow within the closing valve will be essentially inviscid. Only when the closure is almost complete are the cusp boundary-layer thicknesses comparable with the channel width. During closure, as well as during mid-diastole, the vorticity generated within the boundary layers formed on the interior surfaces of the valve cusps will be convected into the ventricle in the form of a vortex sheet surrounding the diastolic jet flow issuing from the valve, but in the quasi-one-dimensional model which we have adopted to describe the closure process the detailed structure of the jet flow into the ventricle is not considered.

Since our experiments indicated that the time history of the circulatory motion within the ventricle was different from that assumed in the Bellhouse model, this aspect of the model was modified. From the pressure-difference measurements discussed earlier, it was determined that a theoretical model in which the pressure and kinetic energy density within the ventricle are uniform in space and a function of time linked to the jet deceleration gives a more accurate, yet simpler estimate of the ventricular stagnation pressure than that predicted by the Hill vortex model. This also appears to be true for the aortic valve.

Whereas the jet issuing from the valve during the opening phase of the motion behaves in a more-or-less two-dimensional fashion, the fluid motion in the ventricle towards the valve during closure is essentially axisymmetric. On the basis of this observation, we adopt a planar model of the valve for the opening process and an axisymmetric model for the closure process. Another assumption which is made is that the vertical height l of the valve is a constant, in order to reduce mathematical complications. Of course, it is true only that the cusp length l_s of the valve is constant. However, we have carried out the analysis both with l constant and with l_s constant and have found that, although the latter analysis is algebraically considerably more complicated than the former, the results are virtually indistinguishable for valves which are not unreasonably short.

The opening process

The geometry for the opening process of the mitral valve is shown in figure 9. The mitral-valve orifice width is $2a$ and the mean velocity across the orifice is u_1. The distance between the cusp margins at the distal end of the valve is $2r$ and the flow velocity through the valve at the distal end is u_2. The breadth of the valve is taken to be b in the direction perpendicular to the plane of the figure.

Conservation of mass flow through the valve under the assumption of constant fluid density ρ gives

$$2abu_1 - 2rbu_2 = d\mathcal{V}/dt, \tag{1}$$

where

$$\mathcal{V} = (a+r)\,lb \tag{2}$$

is the volume of fluid contained within the valve. However, as discussed earlier, it has been observed in our data that $u_1 \doteq u_2$ during valve opening. Using the approximation $u_1 \doteq u_2$ and with

$$\lambda = r/a, \quad S = l/UT, \quad \tau = t/T,$$

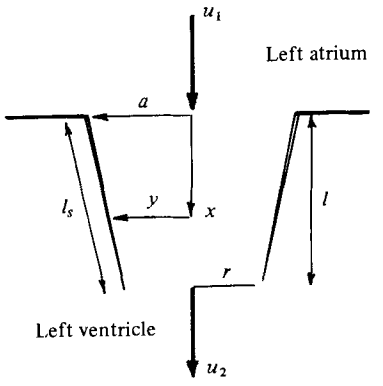

FIGURE 9. Analytical configuration of the planar mitral valve for the opening process.

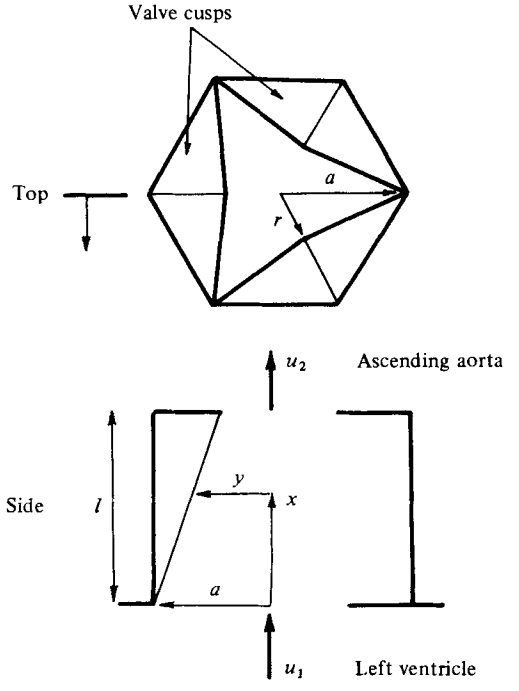

FIGURE 10. Analytical configuration of the aortic valve for the opening process.

where U is the peak velocity through the valve and T the period of the motion, we obtain the following equation for valve opening:

$$\frac{d\lambda}{d\tau} \equiv \lambda' = \frac{2}{S}(1-\lambda)\left(\frac{u_1}{U}\right). \tag{3}$$

Given a knowledge of the Strouhal number S and the time dependence of u_1/U, the valve motion during opening can be calculated from an integration of (3), with initial condition $\lambda = 0$ at $\tau = \tau_0$ (where τ_0 is taken to be the beginning of ventricular diastole).

The opening process for the aortic valve is considered for the different valve geometry shown in figure 10. The distal orifice of the valve is star-shaped and the

proximal one is assumed to be hexagonal for mathematical simplicity. By following the same derivation procedure as was applied in the case of the mitral valve, we get

$$\lambda' = \frac{2}{S}(1-\lambda)\left(\frac{u_1}{U}\right),$$

which is exactly the same as (3). This planar flow relationship was found to predict an opening faster than that predicted by an axisymmetric model (truncated-cone geometry) derived in a similar fashion.

The closure process

The truncated-cone geometry adopted for the closure of the mitral valve is shown in figure 11. It is assumed that the pressure p and the velocity u are uniform across the cross-section of the valve. It is also assumed that the valve cusps are inertialess and the mean ventricular pressure $\bar{p}_v$ acting on the outer surface of the conical valve is equal to the mean pressure on the inner surface of the valve (consistent with our view of the valve as a passive device which 'floats' with the fluid motion).

Conservation of mass yields

$$\pi a^2 u_1 - \pi r^2 u_2 = d\mathscr{V}/dt \tag{4}$$

where

$$y = a - \frac{(a-r)}{l}x$$

and

$$\mathscr{V} = \int_0^l \pi y^2 dx = \tfrac{1}{3}\pi l(a^2 + ar + r^2). \tag{5}$$

From (4) and (5), with the same non-dimensionalization as before,

$$\frac{u_2}{U} = \frac{1}{\lambda^2}\frac{u_1}{U} - \frac{(1+2\lambda)}{3\lambda^2}S\lambda'. \tag{6}$$

Conservation of momentum gives

$$F_x = \frac{\partial}{\partial t}\int_{\mathscr{V}} \rho u \, d\mathscr{V} + \int_A \rho u(\mathbf{q}\,.\,d\mathbf{A}), \tag{7}$$

where

$$F_x = \pi a^2 p_1 - \pi r^2 p_2 - \pi(a^2 - r^2)\bar{p}_v \tag{8}$$

and the velocity integrals are evaluated with the aid of the relation for the velocity at any cross-section x of the valve:

$$u = \frac{a^2}{y^2}u_1 - \frac{dr/dt}{3y^2}\left(\frac{x^2}{l}\right)(a+2y). \tag{9}$$

Using (8) and (9) in (7), we obtain

$$\frac{p_1 - p_2}{\frac{1}{2}\rho U^2} - (1-\lambda^2)\frac{\bar{p}_v - p_2}{\frac{1}{2}\rho U^2} = 2S\left(\frac{u_1}{U}\right)' - \frac{S^2}{3}\lambda''(1+\lambda) + \frac{S^2\lambda'^2}{9\lambda}(2+8\lambda+5\lambda^2)$$
$$+ 2\left(\frac{u_1}{U}\right)^2\left(\frac{1}{\lambda^2} - 1\right) - \frac{4S}{3\lambda^2}\frac{u_1}{U}\lambda'(1+2\lambda), \tag{10}$$

in which, as before, primes denote differentiation with respect to τ.

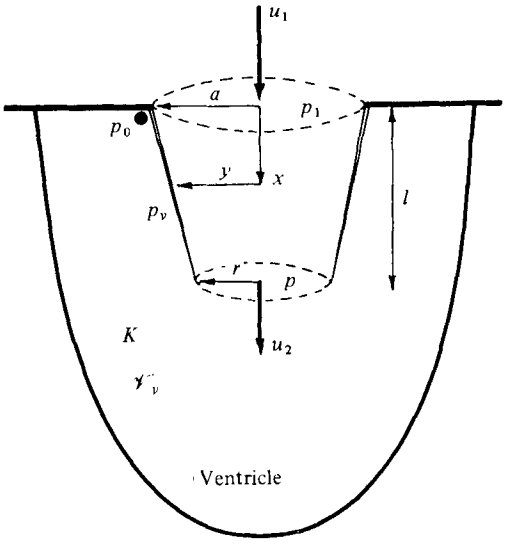

FIGURE 11. Analytical configuration of the axisymmetric mitral valve for the closure process.

Bernoulli's equation along the central streamline of the flow is

$$(p_1+\tfrac{1}{2}\rho u_1^2)-(p_2+\tfrac{1}{2}\rho u_2^2)=\rho\int_0^l \frac{\partial u}{\partial t}\,dx. \tag{11}$$

Using (6) to express u_2 in term of u_1, we obtain

$$\frac{p_1-p_2}{\frac{1}{2}\rho U^2}=\frac{2S}{\lambda}\left(\frac{u_1}{U}\right)'-\frac{2S^2}{3\lambda}\lambda''+\frac{S^2\lambda'^2}{9\lambda^4}(1+4\lambda+10\lambda^2)$$
$$+\left(\frac{u_1}{U}\right)^2\left(\frac{1}{\lambda^4}-1\right)-\frac{2Su_1/U}{3\lambda^4}\lambda'(1+2\lambda+3\lambda^2). \tag{12}$$

Flow within the ventricle

In the closure process, we assume that the kinetic energy per unit mass within the ventricle is uniform in space, a function of time only, and proportional to the peak kinetic energy $\frac{1}{2}U^2$. We assume also that the static pressure in the ventricle is equal to p_2, the pressure at the distal end of the valve. Thus we take the kinetic energy of the ventricular fluid surrounding the jet to be given by

$$(\mathrm{KE})_v=\tfrac{1}{2}K\mathscr{V}_v\rho U^2, \tag{13}$$

where $K(\tau)$ is some function of time and $\mathscr{V}_v$ is the ventricular volume. The stagnation pressure p_0 in the ventricle is given by

$$p_0=p+\tfrac{1}{2}K\rho U^2=p_2+\tfrac{1}{2}K\rho U^2. \tag{14}$$

Conservation of mass for the ventricle gives

$$d\mathscr{V}_v/dt=\pi a^2u_1. \tag{15}$$

Conservation of energy for the ventricle, with $\mathbf{q}$ denoting the fluid vector velocity, is expressed as

$$\frac{\partial}{\partial t}\int_{\mathscr{V}_v}(\tfrac{1}{2}\rho q^2)\,d\mathscr{V}+\int_{A_1}(\tfrac{1}{2}\rho q^2)(\mathbf{q}\,.\,d\mathbf{A})+\int_{A_v+A_1}p\mathbf{q}\,.\,d\mathbf{A}=0. \tag{16}$$

(ventricular volume) (inlet flow area) (ventricular wall area + inlet flow area)

(Viscous terms are neglected because the time period of diastole is too short to allow any extensive dissipation to occur; for example, the diastolic period in our experiments was 1–2 s with saline as the working fluid whereas the characteristic dissipation time l^2/ν is of the order of 100 s if l is taken as 1 cm.) Equation (16) eventually reduces to the differential equation

$$\frac{dK}{d\tau} = \theta(\tau)\left[\frac{p_1 - p_2}{\frac{1}{2}\rho U^2} + \left(\frac{u_1}{U}\right)^2 - K\right], \tag{17}$$

where

$$\theta(\tau) = \frac{u_1/U}{\frac{S\mathcal{V}_i}{\pi a^2 l} + \int_{\tau i}^{\tau}\left(\frac{u_1}{U}\right)d\tau}, \tag{18}$$

in which $\mathcal{V}_i$ is the ventricular volume at τ_i, the time of initiation of valve closure.

Now the mean pressure $\bar{p}_v$ on the valve cusp is assumed to be the average of the stagnation pressure p_0 (see figure 11) at the base of the valve and the pressure p_2 at the cusp tip:

$$\bar{p}_v = \tfrac{1}{2}(p_0 + p_2) = p_2 + \tfrac{1}{2}(\tfrac{1}{2}K\rho U^2),$$

so that

$$(\bar{p}_v - p_2)/\tfrac{1}{2}\rho U^2 = \tfrac{1}{2}K. \tag{19}$$

Substitution of (19) and (12) into (10) yields the differential equation

$$\lambda^2 S^2(2+\lambda)\lambda'' = -\tfrac{3}{2}\lambda^4(1+\lambda)K + 6S\lambda^3\left(\frac{u_1}{U}\right)' + 3(1+\lambda)^2(1-\lambda)\left(\frac{u_1}{U}\right)^2$$
$$- 2S\left(\frac{u_1}{U}\right)\lambda'(1+3\lambda+4\lambda^2) + \tfrac{1}{3}S^2\lambda'^2(1+5\lambda+13\lambda^2+5\lambda^3). \tag{20}$$

Equations (17) and (20) are two simultaneous ordinary differential equations relating the mitral orifice flow u_1/U to the valve closure process, expressed in terms of $\lambda(\tau)$. With u_1/U measured from experiments, the initial conditions for the numerical integration of these equations are taken from the valve opening model; at $\tau = \tau_i$, say $\lambda = \lambda_i$, $\lambda' = \lambda_i'$ and in most cases the matching time τ_i is taken when $\lambda_i = 0{\cdot}99$ and λ_i', $\lambda_i'' \doteq 0$. The initial value for K (which is very close to zero) at closure is calculated from (20) with λ_i, λ_i' and λ_i'' taken from the opening process. This is in contrast to the Bellhouse assumption that a Hill-type vortex flow fills the ventricle throughout the entire period of diastole. Although the Bellhouse analysis and the present one are very similar, they do differ in one important respect. In the Bellhouse & Bellhouse (1972) analysis the ventricular vortex contributes a pressure difference across the valve cusps throughout most of diastole, including a portion of the time interval when the valve is fully open and effectively motionless. This can be seen from figure 10 of their paper. In the present analysis, because K is essentially zero at the start of valve closure, a pressure difference does not appear across the valve cusps until the onset of flow deceleration. This behaviour seems to be in better accord with experimental observations, as seen from figure 7, and results in an improved prediction of valve motion.

In the case of aortic-valve motion, we assume that $\bar{p}_v \doteq p_2$ (i.e. $K \doteq 0$). This is a reasonable assumption because, unlike the flow rushing into the enclosed ventricle

during diastole in the case of the mitral valve, the flow entering the aortic sinuses is usually a small fraction of that passing through the aortic valve. For this reason, we expect negligible kinetic energy recovery in the sinuses and therefore practically no pressure variation in them. (This assumption is consistent with the Snuggs & Aggarwal (1975) experiment, in which no significant pressure variation was recorded inside their semi-cylindrical hollow under steady and unsteady flow.) The assumption $K = 0$ leads to the elimination of (17) altogether, and the first term on the right-hand side of (20) drops out.

4. Results predicted by the present theory

Computer analyses were performed using the present theory to calculate valve motion from experimental trans-valvular flow, and also to study the influence of several important parameters involved in the closure process.

The improvement of the present theory over the Bellhouse & Bellhouse theory is clearly demonstrated in figures 12, 13 and 14, in which part (*a*) gives the measured valve orifice velocities and part (*b*) shows the comparisons between valve motions measured in the experiments, those predicted by the Bellhouse & Bellhouse theory and those calculated using the present theoretical model. Figures 12 and 13 are plots of mitral and aortic data, respectively, taken from the Bellhouse & Bellhouse reports (1972, 1969). Figure 14 shows an example of the data obtained in the present studies. One can observe in these figures the good agreement between valve motions computed using our theoretical model and those obtained from the experimental measurements.

From the present theory it is evident that the mitral velocity, flow deceleration, maximum valve opening position, Strouhal number and size of the ventricle might exert some influences on valve closure. To study theoretically these influences on the efficiency of valve closure, as represented by the amount of regurgitation, we also performed a numerical analysis using simple models for the time variation in mitral orifice velocity.

The effect of mitral flow and flow deceleration

We assume a flow deceleration model of the form

$$u_1/U = A - B\tau,$$

where A represents the initial mitral orifice velocity at $\tau = 0$ and B is the magnitude of the deceleration. The initial conditions (at $\tau = 0$) are assumed to be $\lambda = 1$, $\lambda' = 0$ and $K = 0$ with the Strouhal number fixed at 0·03, which is typical for the human heart. The mitral orifice radius a was 1·27 cm, the valve length l was 1·79 cm and the volume before deceleration was 100 ml. The dimensionless regurgitation R is calculated from the formula

$$R = \int_{\tau_1}^{\tau_2} \left(\frac{u_1}{U}\right) d\tau,$$

where τ_1 is the time at which the velocity passed through zero and τ_2 is the time when the valve closure was complete. Since the velocity function is known and the valve motion has been computed using the theory, τ_1 and τ_2 can be easily obtained from this information.

Figure 15 shows the results of this theoretical study. It is apparent that an increase

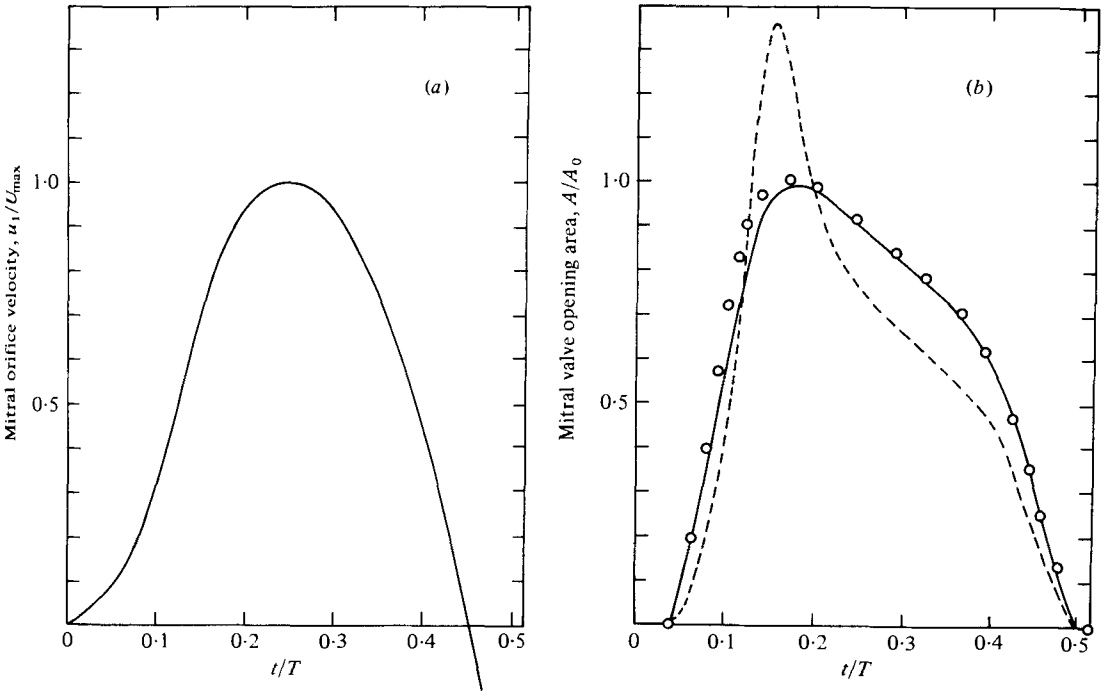

FIGURE 12. (*a*) Time-dependent mitral orifice velocity measured in the Bellhouse & Bellhouse experiment (1972). (Period $T = 2{\cdot}5$ s; peak velocity $U_{max} = 50$ cm/s.) (*b*) Time-dependent mitral-valve motion. ○, data obtained from the Bellhouse & Bellhouse experiment (1972); – – –, motion calculated using the Bellhouse & Bellhouse theory (1972); ——, motion computed using the present theoretical model. (End-systolic volume = 107 ml; orifice area $A_0 = 5{\cdot}07$ cm².)

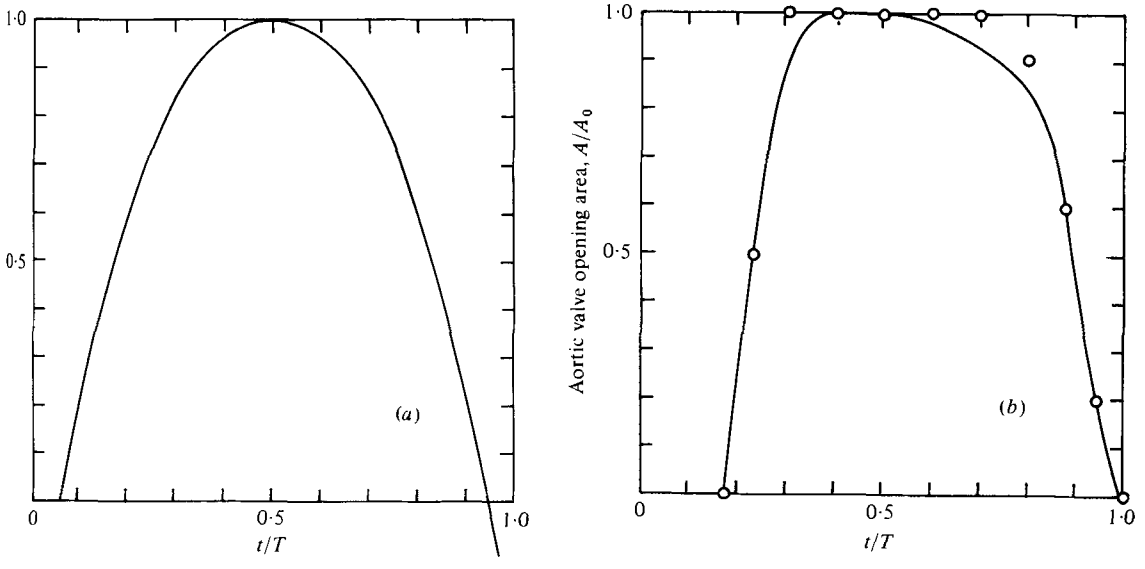

FIGURE 13. (*a*) Time-dependent aortic orifice velocity measured in the Bellhouse & Bellhouse experiment (1969). (Period $T = 0{\cdot}44$ s; peak velocity $U_{max} = 71{\cdot}2$ cm/s.) (*b*) Time-dependent aortic-valve motion. ○, data obtained from the Bellhouse & Bellhouse experiment (1969); ——, motion computed using the present theoretical model. (Orifice area $A_0 = 5{\cdot}07$ cm².)

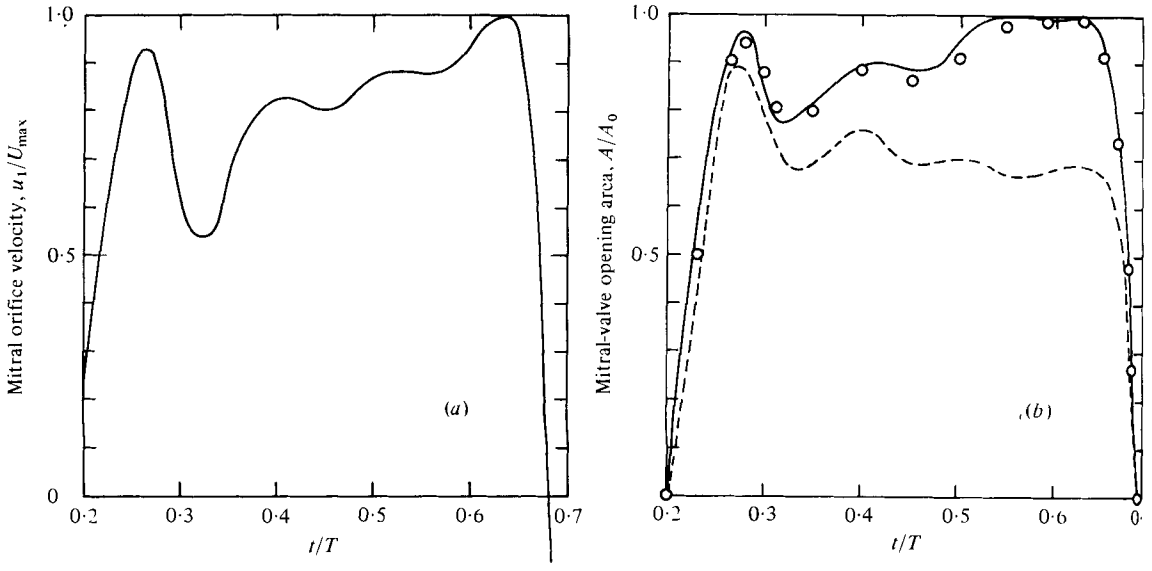

FIGURE 14. (*a*) Time-dependent mitral orifice velocity measured in the present study. (Period $T = 3{\cdot}0$ s; peak velocity $U_{max} = 17{\cdot}68$ cm/s.) (*b*) Time-dependent mitral-valve motion. ○, experimental data from the present study; – – –, motion calculated using the Bellhouse & Bellhouse theory (1972); ——, motion computed using the present theoretical model. (Orifice area $A_0 = 5{\cdot}07$ cm^2.)

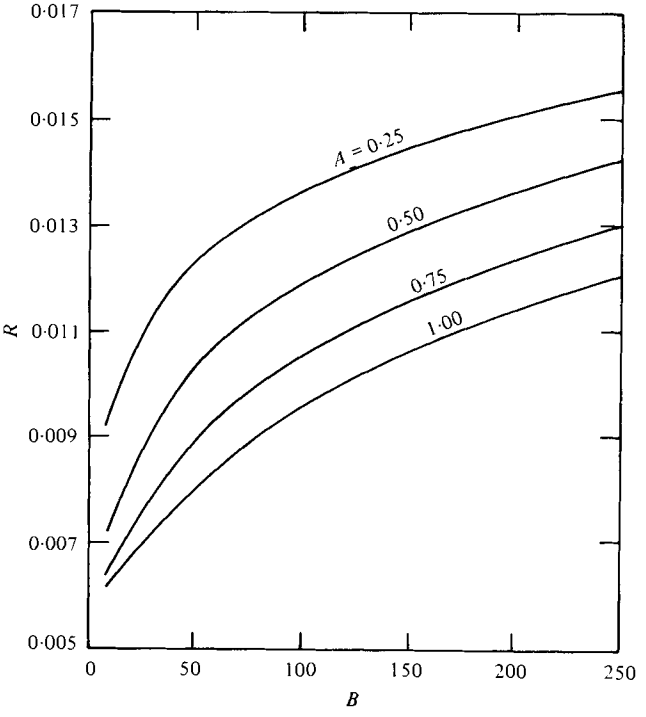

FIGURE 15. Effect of flow deceleration B on mitral regurgitation R for various initial mitral velocities A.

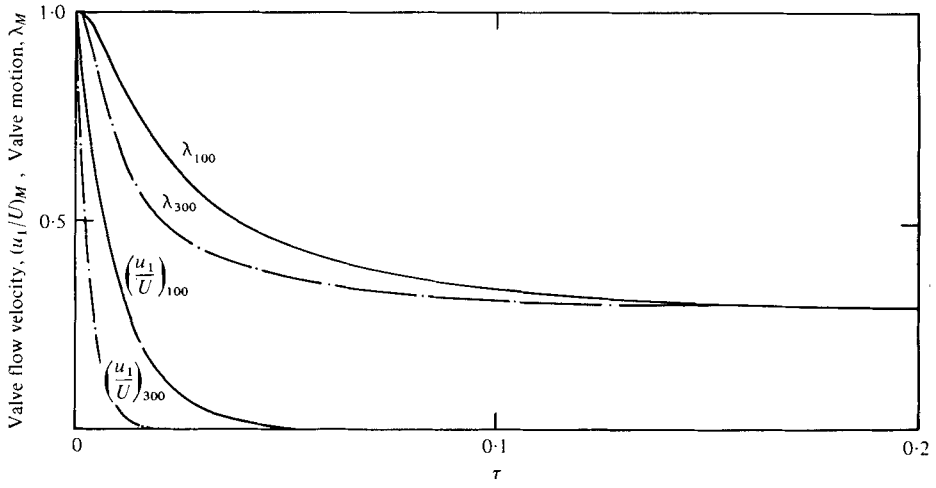

FIGURE 16. Valve motions λ_M computed from theoretical mitral orifice velocity $(u_1/U)_M = \exp(-M\tau)$ with $M = 100$ and 300 respectively.

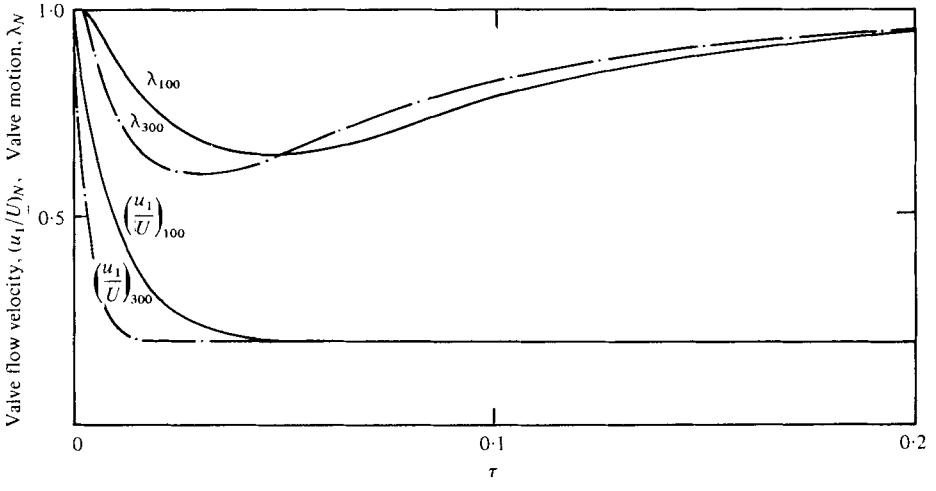

FIGURE 17. Valve motions λ_N computed from theoretical mitral orifice velocity $(u_1/U)_N = 0{\cdot}2 + 0{\cdot}8\exp(-N\tau)$ with $N = 100$ and 300 respectively.

in B or a decrease in A leads to additional regurgitation during valve closure. This finding is consistent with our experimental observations; when the stroke volume was reduced, reflecting a lowered mitral velocity, or when the heart rate became higher, producing a stronger deceleration, the reverse flow recorded during valve closure was evidently intensified.

To investigate the deceleration effect on valve motion, two velocity models with an exponentially decreasing characteristic were postulated:

$$(u_1/U)_M = e^{-M\tau} \quad \text{(flow deceleration to zero)}$$

and

$$(u_1/U)_N = 0{\cdot}2 + 0{\cdot}8e^{-N\tau} \quad \text{(flow deceleration to the value 0·2).}$$

where M and $0{\cdot}8N$ reflect the initial flow deceleration at $\tau = 0$. The corresponding theoretical valve motions $\lambda_M(\tau)$ and $\lambda_N(\tau)$ for $M = 100$ and 300 and $N = 100$ and 300 are plotted in figures 16 and 17 respectively. It is clear that the deceleration influence exerted on valve motion during closure is a transient action occurring only at higher flow decelerations. When the mitral velocity has decreased to zero in the first case, the valve cusps are closed only to about 30 % of the orifice radius. In the second case, where the flow velocity decreases towards an asymptotic value of 0·2, valve reopening is evident even though the velocity is still decreasing.

The convergent valve

If the valve cone is somehow restricted from opening fully, such as in the case of valvular stenosis, a very interesting result can be illustrated from the theoretical analysis. The same linear model $u_1/U = A - B\tau$ for mitral velocity is employed, except that the initial condition for valve closing is now $\lambda = 0{\cdot}5$ at $\tau = 0$.

Figure 18 shows the dimensionless regurgitation R as a function of both the flow deceleration B and the initial mitral velocity A. At higher values of B, R remains at fairly low values regardless of the variation in A. However, at low values of B dramatic increases in R are apparent, although a decrease in A seems to reduce R considerably. In the case of the physiological valve, the dimensionless flow deceleration B is estimated to be between 5 and 50. With this estimation and from figure 18, one can see that a significant amount of regurgitation could occur during valve closure for a stenotic convergent valve. One should note that this is a fluid-dynamical consequence rather than one due to a change in valve cusp flexibility. (Of course, thickening of valve cusps would also hinder valve functioning.)

The effect of Strouhal number and ventricular volume

In this investigation, we assume the mitral orifice velocity to be of the form

$$u_1/U = 1 - B\tau$$

with the initial conditions $\lambda = 1$, $\lambda' = 0$ and $K = 0$ at $\tau = 0$. The initial ventricular volume $\mathscr{V}_0$ is made dimensionless by the factor $\pi a^2 l$, which is the volume bounded by the fully open valve cusps, thus $\mathscr{V}_n = \mathscr{V}_0/\pi a^2 l$.

To examine the volume effect, valve motion is calculated from the theory assuming $S = 0{\cdot}01$, $B = 10$ and 100 and using the assumed mitral velocity as input data. The results shown in figure 19 indicate that enlargement of the ventricular volume would delay the valve closure only at low flow decelerations, and no appreciable effect can be seen when the flow deceleration is strong. One can also see that at low flow decelerations the actual delay in complete valve closure is relatively small since the closing velocity of valve cusps at late diastole increases to compensate for the delay during early closure.

The regurgitation during valve closure was also computed as a function of S and $\mathscr{V}_n$ for a given value of B (figure 20). It is evident that, in general, an increase in S would lead to a rise in regurgitation, whereas the volume effect (three orders of magnitude in volume variation from 1 to 1000) has little influence on the amount of reverse flow. However, at lower values of B the variation in backflow volume, in response to a change in ventricular volume, tends to increase slightly.

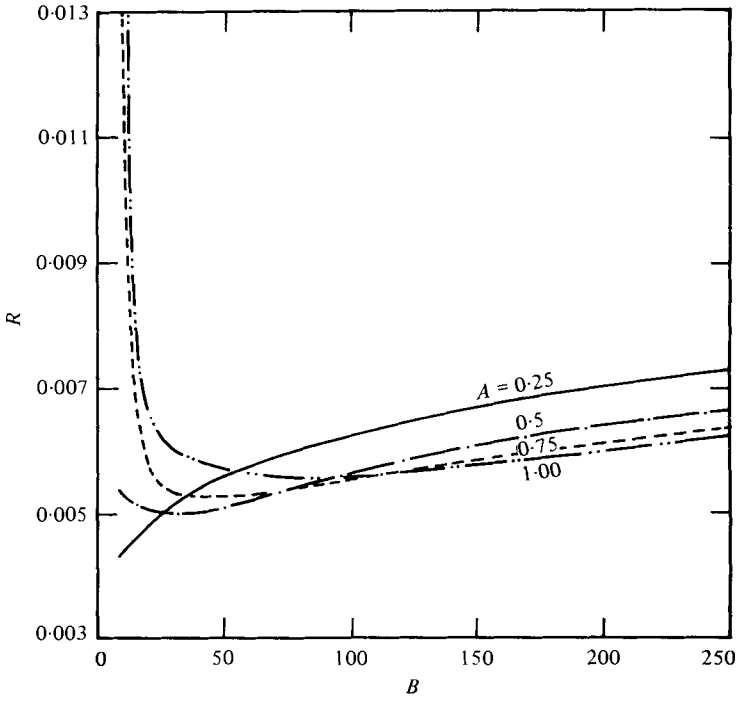

FIGURE 18. Effect of flow deceleration B and initial mitral velocity A on mitral regurgitation R for a convergent mitral valve.

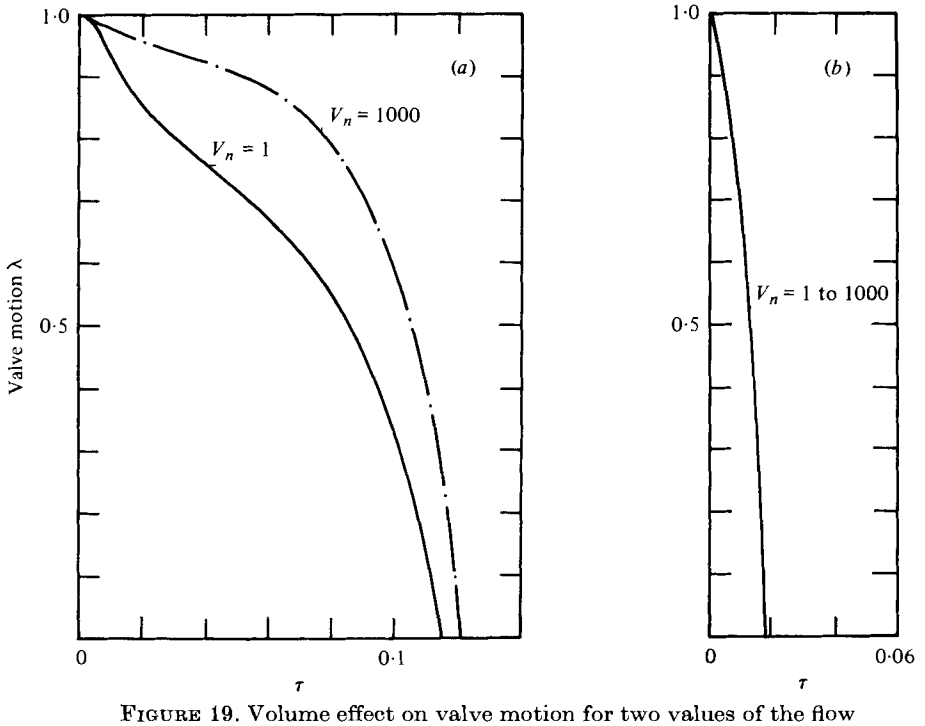

FIGURE 19. Volume effect on valve motion for two values of the flow deceleration: (*a*) $B = 10$; (*b*) $B = 100$.

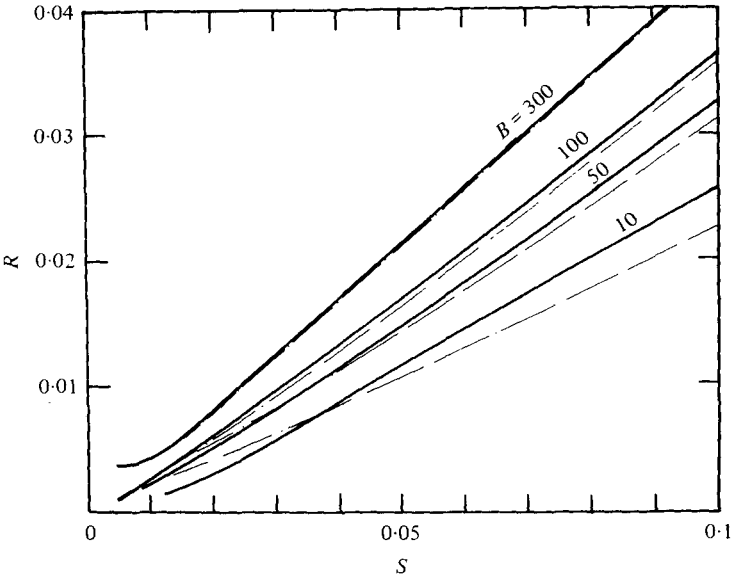

FIGURE 20. Effect of Strouhal number S on mitral regurgitation R for various values of the flow deceleration B and ventricular volume V_n. ——, $V_n = 1$; —·—, $V_n = 1000$.

All these theoretical findings agree qualitatively with the experimental results reported earlier.

5. Conclusions

The experimental and theoretical studies presented have provided a better understanding of heart-valve dynamics associated with trans-valvular flow. We believe that the motion of a healthy human heart valve depends mainly on the fluid motion passing between its cusps, although, in the case of the atrioventricular valves, it also responds slightly to the force contributed by the kinetic energy recovery process within the ventricle.

In the acceleration phase of the valve flow, valve cusps open to a position nearly parallel to the essentially unidirectional jet issuing from the orifice. Hence no restraints are necessary to prevent the valve cusps from opening too far during ventricular diastole.

The primary mechanism for efficient valve closure is the adverse pressure gradient related to the deceleration of the valve flow. The size of the ventricle has little dynamical effect on valve efficiency, although it slightly affects the closure movement of the valve at low flow decelerations.

In the theoretical studies, we have shown that it is possible to modify the Bellhouse & Talbot theory for practical application. The mathematical analysis, which accurately predicts valve motion from experimental valve flow, also gives detailed qualitative descriptions of the influences produced by major physical parameters. In particular, a reason for the increase in regurgitation of a stenotic valve was illustrated. Other clinical applications of the theory will be reported subsequently.

This work was supported by the National Science Foundation under Grant No. ENG-73-03970.

REFERENCES

BELLHOUSE, B. J. & BELLHOUSE, F. H. 1969 *Circulation Res.* **25**, 693.

BELLHOUSE, B. J. & BELLHOUSE, F. H. 1971 The fluid mechanics of a model mitral valve and left ventricle. *Oxford Univ. Engng Sci. Lab. Rep.* no. 1013/71.

BELLHOUSE, B. J. & BELLHOUSE, F. H. 1972 *Cardiovasc. Res.* **6**, 199.

BELLHOUSE, B. J., BELLHOUSE, F. H., ABBOTT, J. A. & TALBOT, L. 1973 *Cardiovasc. Res.* **4**, 490.

BELLHOUSE, B. J. & TALBOT, L. 1969 *J. Fluid Mech.* **35**, 721.

HENDERSON, Y. & JOHNSON, F. E. 1912 *Heart* **4**, 69.

LEE, C. S. F. 1977 Fluid mechanical study of mitral valve motion. Ph.D. thesis, Mechanical Engineering Dept., University of California, Berkeley (*U.C. Rep.* no. FM-77-1).

NETTER, F. H. 1969 *The Ciba Collection of Medical Illustrations*, vol. 5. *Heart*. CIBA, Summit, N.Y.

PESKIN, C. S. 1972 Flow patterns around heart valves. Ph.D. thesis, Albert Einstein College of Medicine, Yeshiva University, New York.

SNUGGS, T. A. & AGGARWAL, J. K. 1975 Steady and unsteady flow in a semi-cylindrical hollow. *Oxford Univ. Engng Sci. Lab. Rep.* no. 1118/75.

SPAAN, J. A. E., VAN STEENHOVEN, A. A., VAN DER SCHAAR, P. J., VAN DONGEN, M. E. H., SMULDERS, P. T. & LELIVELD, W. H. 1975 *Trans. Am. Soc. Artif. Int. Organs* **21**, 396.

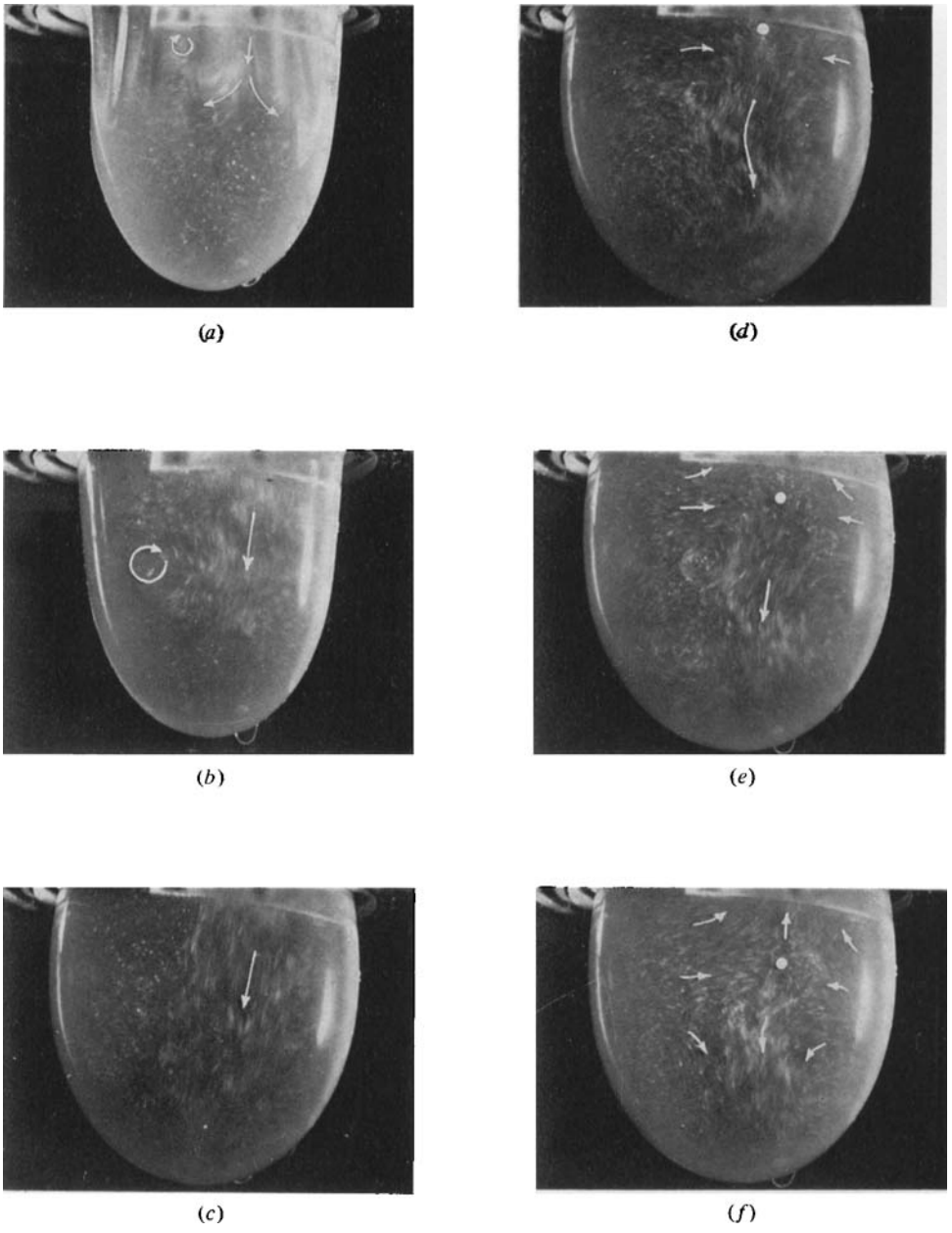

FIGURE 5. Sequential photographs of flow patterns inside model ventricle without a mitral valve. (*a*) $t = 200$ ms, (*b*) $t = 500$ ms, (*c*) $t = 1600$ ms, (*d*) $t = 1900$ ms, 250 ms after the onset of flow deceleration, (*e*) $t = 1950$ ms, (*f*) $t = 2000$ ms, at onset of ventricular systole. (t = time measured with respect to onset of ventricular diastole; white dot indicates approximate location of a stagnation point; white arrows indicate directions of flow.)

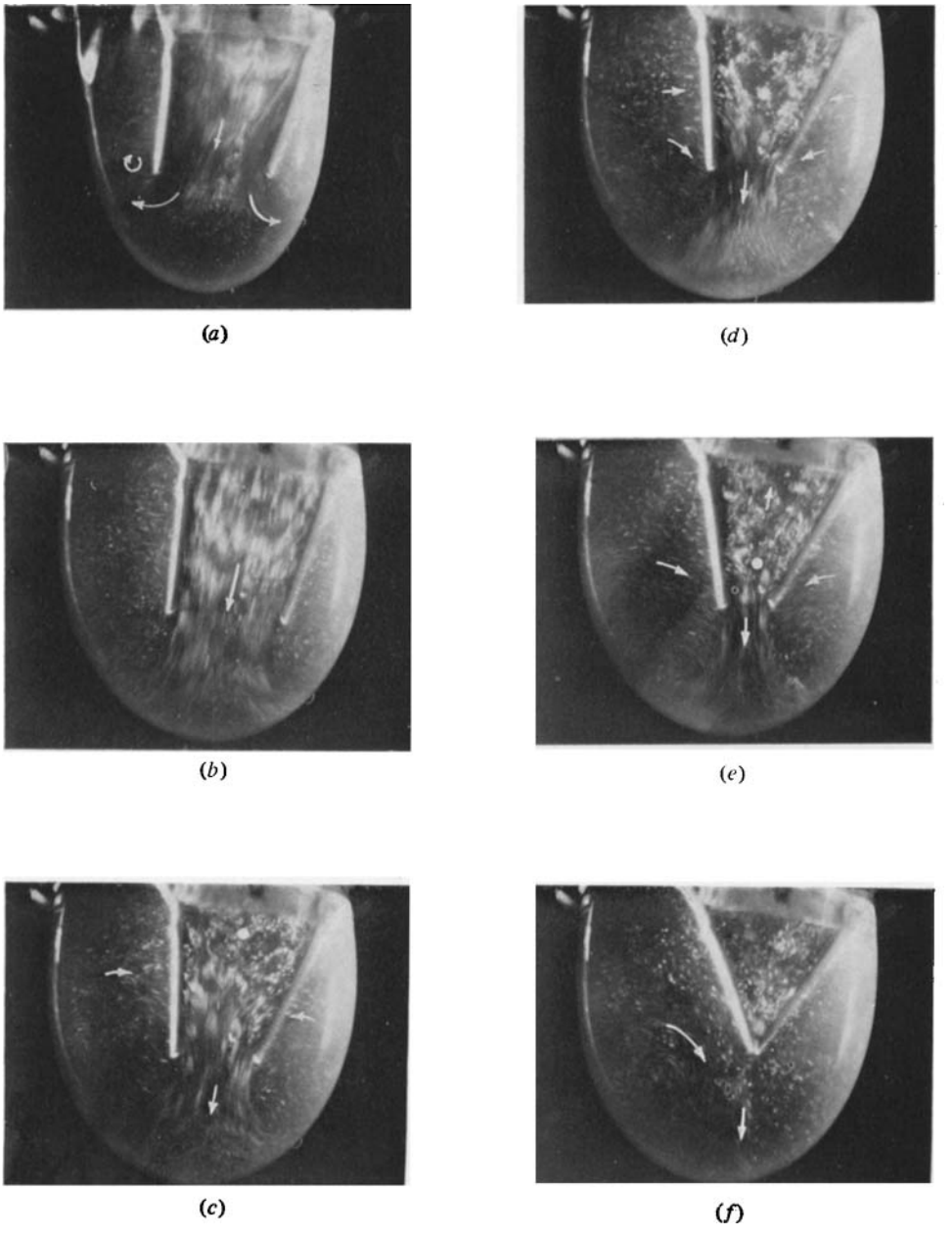

FIGURE 6. Sequential photographs of flow patterns inside model ventricle with a mitral valve. (*a*) $t = 800$ ms, (*b*) $t = 1600$ ms. (*c*) $t = 1800$ ms, 150 ms after the onset of flow deceleration, (*d*) $t = 1850$ ms, (*e*) $t = 1900$ ms, (*f*) $t = 1950$ ms, 50 ms before onset of ventricular systole. (Symbols same as in figure 5.)